JOURNAL OF VIROLOGY, June 2002, p. 5937–5948 Vol. 76, No. 12
0022-538X/02/$04.00+0 DOI: 10.1128/JVI.76.12.5937–5948.2002

Murine Coronavirus Replication-Induced p38 Mitogen-Activated Protein Kinase Activation Promotes Interleukin-6 Production and Virus Replication in Cultured Cells

Sangeeta Banerjee,[1,2]† Krishna Narayanan,[1,2] Tetsuya Mizutani,[1]‡ and Shinji Makino[1,2]*

Department of Microbiology and Immunology, The University of Texas Medical Branch at Galveston, Galveston, Texas 77555-1019,[1] and Department of Microbiology and Institute of Molecular and Cellular Biology, The University of Texas at Austin, Austin, Texas 78712-1095[2]

Received 13 November 2001/Accepted 13 March 2002

Analyses of mitogen-activated protein kinases (MAPKs) in a mouse hepatitis virus (MHV)-infected macrophage-derived J774.1 cell line showed activation of two MAPKs, p38 MAPK and c-Jun N-terminal kinase (JNK), but not of extracellular signal-regulated kinase (ERK). Activation of MAPKs was evident by 6 h postinfection. However, UV-irradiated MHV failed to activate MAPKs, which demonstrated that MHV replication was necessary for their activation. Several other MHV-permissive cell lines also showed activation of both p38 MAPK and JNK, which indicated that the MHV-induced stress-kinase activation was not restricted to any particular cell type. The upstream kinase responsible for activating MHV-induced p38 MAPK was the MAPK kinase 3. Experiments with a specific inhibitor of p38 MAPK, SB 203580, demonstrated that MHV-induced p38 MAPK activation resulted in the accumulation of interleukin-6 (IL-6) mRNAs and an increase in the production of IL-6, regardless of MHV-induced general host protein synthesis inhibition. Furthermore, MHV production was suppressed in SB 203580-treated cells, demonstrating that activated p38 MAPK played a role in MHV replication. The reduced MHV production in SB 203580-treated cells was, at least in part, due to a decrease in virus-specific protein synthesis and virus-specific mRNA accumulation. Interestingly, there was a transient increase in the amount of phosphorylation of the translation initiation factor 4E (eIF4E) in infected cells, and this eIF4E phosphorylation was p38 MAPK dependent; it is known that phosphorylated eIF4E enhances translation rates of cap-containing mRNAs. Furthermore, the upstream kinase responsible for eIF4E phosphorylation, MAPK-interacting kinase 1, was also phosphorylated and activated in response to MHV infection. Our data suggested that host cells, in response to MHV replication, activated p38 MAPK, which subsequently phosphorylated eIF4E to efficiently translate certain host proteins, including IL-6, during virus-induced severe host protein synthesis inhibition. MHV utilized this p38 MAPK-dependent increase in eIF4E phosphorylation to promote virus-specific protein synthesis and subsequent progeny virus production. Enhancement of virus-specific protein synthesis through virus-induced eIF4E activation has not been reported in any other viruses.

Viral infection alters the host cell environment by generating stimuli to which the infected host cell responds. A well-known virus-induced stimulus is the double-stranded RNA (dsRNA) structure produced during viral replication. Host cells have evolved two complementary systems to detect and respond to dsRNA: the 2-5A system and activation of the dsRNA-activated protein kinase PKR (21, 55). In addition, replication of certain viruses in permissive cells activates signaling cascades, which result in the activation of the mitogen-activated protein kinase (MAPK) superfamily. In mammalian cells, four distinct subgroups of MAPK families have been identified: extracellular signal-regulated kinase (ERK1/2), ERK5/big MAPK, c-Jun N-terminal kinase (JNK), and p38-Hog (28, 45). Unlike ERK1/2, which are mostly activated by hormones and growth factors, the JNKs and p38 are most potently activated by proinflammatory cytokines, endotoxins, and environmental stresses such as osmotic shock and heat shock, UV irradiation, or treatment with nucleic acid-damaging agents (22). Thus, JNKs and p38 are also known as stress-activated protein kinases (SAPKs) (22). Each MAPK family consists of a hierarchy of three sequential, dual-specificity kinases: MKKK (MAPKKK or MEKK), MKK (MAPKK or MEK), and MAPK (ERK, JNK, or p38). Upon stimulation, the MKKK is dually phosphorylated on specific residues by cellular signaling molecules. This activated MKKK then phosphorylates the MKK which, in turn, phosphorylates the MAPK on appropriate threonine and tyrosine residues, resulting in activation of the pathway (11, 22). Activated MAPKs have numerous substrates, like transcription factors or downstream kinases, and phosphorylation and activation of these downstream substrates ultimately alters gene expression, thereby manifesting the biological consequences of MAPK activation (67). In spite of the growing body of evidence for virus infections triggering MAPK pathways (45), very little is known about the role that activated MAPK pathways play in virus replication and propagation.

Coronaviruses are large, enveloped, positive-strand RNA viruses associated with a wide variety of diseases in both ani-

* Corresponding author. Mailing address: Department of Microbiology and Immunology, The University of Texas Medical Branch at Galveston, Galveston, TX 77555-1019. Phone: (409) 772-2323. Fax: (409) 772-5065. E-mail: shmakino@utmb.edu.

† Present address: Department of Cell and Developmental Biology, Oregon Health Sciences University, Portland, OR 97201.

‡ Present address: Department of Environmental Veterinary Sciences, Graduate School of Veterinary Medicine, Hokkaido University, Hokkaido, Japan.

mals and humans (66). Mouse hepatitis virus (MHV) is one of the most well-characterized coronaviruses. After MHV infection, MHV RNA synthesis, which involves synthesis of a genome-length, negative-strand RNA template (2, 4, 42) and subsequent synthesis of seven, mature mRNA species (31), takes place in the cytoplasm. MHV particles, which contain three envelope proteins (S, M, and E) and an internal helical nucleocapsid, which consists of N protein and genomic RNA, buds from internal cellular membranes (25, 37, 61). Extensive morphological, physiological, and biological changes occur in cells infected with MHV (1, 3, 15, 54, 58, 59). Examination of various MHV-induced biological changes in infected cells is important in understanding the mechanisms of coronavirus-induced diseases. However, our knowledge of various MHV-host cell interactions, including the status of stress pathways in infected cells, is still in its infancy.

In the present study, we demonstrated p38 MAPK activation for extended time periods after MHV infection and identified proteins phosphorylated in a p38 MAPK-dependent manner in the context of viral infection. Furthermore, we showed that activated p38 MAPK affected MHV replication, particularly at the step of viral mRNA synthesis and viral protein translation, at least partly, if not completely, through p38 MAPK-mediated phosphorylation of translation initiation factor 4E (eIF4E).

MATERIALS AND METHODS

Antibodies. All phospho-specific antibodies and phosphorylation-state-independent antibodies for p38, JNK, ERK, MKK3, and eIF4E were purchased from Cell Signaling Technology (Beverly, Mass.). Phospho-specific antibody for MAPK-interacting kinase 1 (Mnk1) was purchased from Cell Signaling Technology, and the phosphorylation-state-independent antibody for Mnk1 was from Santa Cruz Biotechnology (Santa Cruz, Calif.).

Cell culture and viruses. J774.1 cells (58) and 17Cl-1 cells (1, 56) were grown in Dulbecco's modified essential medium (Gibco-BRL) supplemented with 10% fetal bovine serum. L929 cells were grown in Eagle minimal essential medium (Sigma) supplemented with 10% fetal bovine serum. DBT, an astrocytoma cell line (16), was maintained in minimal essential medium supplemented with 8% newborn calf serum and 10% tryptose phosphate broth. Antibiotics were supplemented in the media of all cell cultures. For preparation of the stock virus sample, the plaque-cloned A59 strain of MHV (MHV-A59) was propagated in DBT cells, as previously described (30). Virus infectivity was determined by plaque assay by using DBT cells (16).

Virus infections and drug treatments. Cultured cells (3×10^5 cells) were grown in 35-mm dishes for 48 h prior to MHV infection. MHV was added to the cell culture at a multiplicity of infection (MOI) of 20. After a 1-h incubation at 37°C, the virus inoculum was removed. To reduce endogenous levels of activated MAPKs, fresh basal medium without growth factors, i.e., serum, was added to the culture. SB 203580 (4-[4-fluorophenyl]-2-[4-methylsulfinylphenyl]-5-[4-pyridyl] imidazole) was purchased from Calbiochem (La Jolla, Calif.) and stored as a 20 mM stock solution in dimethyl sulfoxide (DMSO) at −20°C. For the experiments examining virus protein synthesis and RNA synthesis, a water-soluble form of SB 203580 was used; both drugs are functionally identical. Where indicated, SB 203580 was diluted to 20 μM in cell culture medium and added to cultures 1 h prior to infection. Inhibitor was not included in the virus inoculum. After 1 h of virus adsorption, the virus inoculum was removed and fresh basal medium containing fresh inhibitor was added to the culture.

Western blot analyses. At various times postinfection (p.i.), culture supernatant was removed and cells were directly lysed into sodium dodecyl sulfate (SDS) sample buffer (62.5 mM Tris-HCl [pH 6.8], 2% SDS, 10% glycerol, 50 mM dithiothreitol, 0.1% bromophenol blue). Samples were boiled, and proteins were separated by SDS–12% polyacrylamide gel electrophoresis (PAGE). Proteins were blotted onto polyvinylidene difluoride membranes, and the immunoblots were processed with phospho-specific antibodies. The blots were stripped and reprobed with phosphorylation-state-independent antibodies. For eIF4E analysis, cells were directly lysed in lysis buffer (containing 10 mM HEPES [pH 7.2], 5 mM EDTA, 1% Triton X-100, 150 mM NaCl, 20 mM NaF, 20 mM sodium pyrophosphate, 20 mM β-glycerophosphate, and 20 mM sodium molybdate and supplemented with kinase, phosphatase, and protease inhibitors) (14). The relative level of phosphorylation of each phospho-protein was determined by quantitative densitometry. The signals from each of the phospho-specific immunoblots were normalized against the individual total protein amounts. The fold increase of the phospho-specific signal over the signal at 0 h p.i. was calculated.

p38 MAPK assay. The activity of p38 MAPK was analyzed by using a p38 MAPK assay kit (p38 MAPK assay kit [catalog no. 9820]; Cell Signaling Technology). Phosphorylated p38 was immunoprecipitated with a p38-phospho-specific antibody from 200 μg of lysate; this antibody specifically recognized phosphorylated p38 and did not cross-react with phosphorylated JNK or ERK1/2. The immune complex was washed thoroughly and resuspended in kinase buffer containing ATP and 1 μg of recombinant activating factor-2 (ATF-2) as a p38 MAPK substrate. The reaction was incubated at 30°C for 45 min and terminated by adding SDS sample buffer. The kinasing reaction was analyzed by Western blotting with a phospho-specific anti-ATF-2 antibody.

Quantitation of released IL-6. Supernatants from control cells or infected cells were harvested at 24 h p.i. and clarified by centrifugation (12,000 rpm for 5 min). Release of interleukin-6 (IL-6) was determined by mouse IL-6-specific enzyme-linked immunosorbent assay (ELISA) assay kit (Biosource International, Camarillo, Calif.).

Protein synthesis analysis and Northern (RNA) blotting. Intracellular proteins were labeled, extracted, and separated by SDS-PAGE as previously described (23). Briefly, mock-infected and MHV-infected cells were incubated in methionine-cysteine-free medium for 0.5 h before labeling. Cells were labeled with 75 μCi of Tran^{35}S-label (ICN)/ml, a mixture of ^{35}S-labeled methionine and cysteine, for 30 min at various times p.i. Labeled cells were lysed in lysis buffer (1% Triton-X, 0.5% sodium deoxycholate, and 0.1% SDS in phosphate-buffered saline), and the postnuclear supernatant was separated by SDS-PAGE. Northern blot analysis of MHV-specific RNAs was performed as described previously (38), with a digoxigenin (DIG)-labeled, random-primed probe corresponding to the 3′ end of MHV genomic RNA and visualized by using the DIG Luminescence Detection kit (Boehringer).

LDH assay for drug cytotoxicity. To assess the cytotoxicity of SB 203580, the lactate dehydrogenase (LDH)-based, in vitro toxicology assay kit (Sigma Aldrich, St. Louis, Mo.) was used. Serial 10-fold dilutions of SB 203580 were added to cells and incubated for 24 h. Cell-free supernatant from treated samples were assayed for the amount of LDH activity, which was correlated to cell viability and membrane integrity. The percentage of viable cells was calculated according to the following formula: [(LDH released from treated cells) − (LDH released from untreated cells)/(total LDH released from lysed cells)] × 100.

RESULTS

Activation of SAPKs in MHV-infected cultured cells. We examined whether MHV replication induced p38 MAPK activation in four MHV-susceptible cell lines: DBT (an astrocytoma-derived cell line), 17Cl-1 (transformed NIH 3T3 cells), L929 (fibroblast cells), and J774.1 (a macrophage-derived cell line). These cells were inoculated with MHV at an MOI of 20, and cell extracts were prepared at various times p.i. Extracts from mock-infected cells were used as negative controls (Fig. 1, labeled Mk). Western blot analysis showed an increase in the amount of phosphorylated p38 in 17Cl-1 cells, DBT cells, and J774.1 cells (Fig. 1), whereas the kinetics and extent of phosphorylation differed among these cell lines. In 17Cl-1 cells, a clear increase in the amount of phosphorylated p38 was detected at 8 h p.i., and a high level of phosphorylated p38 was detected until 12 h p.i., the end point of this experiment (Fig. 1A). Phosphorylation of p38 was prominent in DBT and J774.1 cells. In DBT cells, the amount of phosphorylated p38 increased by 10 h p.i., and it became maximal around 12 to 14 h p.i., and then it gradually declined to the basal level by 20 h p.i. (Fig. 1C). In J774.1 cells, a clear increase in the amount of phosphorylated p38 occurred as early as 6 h p.i. Its maximal accumulation occurred by 8 h p.i., and then the amount of phosphorylated p38 gradually declined to basal levels by 16 h p.i. (Fig. 1D). By 24 h p.i., the level of phosphorylated p38

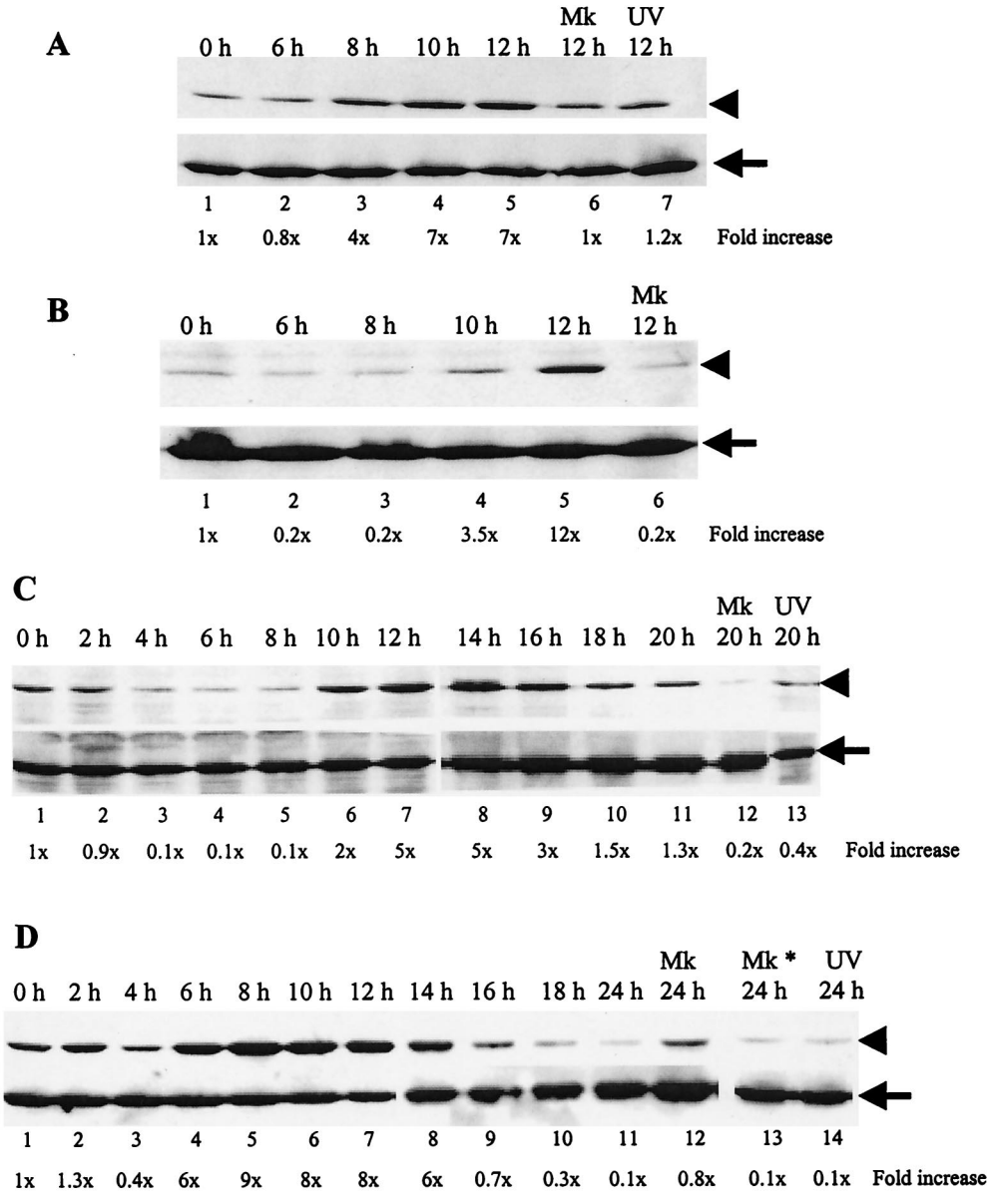

FIG. 1. Phosphorylation of p38 MAPK in MHV-infected 17Cl-1 (A), L929 (B), DBT (C), and J774.1 (D) cells. Cells were infected with MHV at an MOI of 20 (A, C, and D) or 100 (B). Cell extracts were prepared at the indicated times p.i. Western blot analysis with a p38-phospho-specific antibody (upper panels in A to D) demonstrates p38 MAPK that is dually phosphorylated at residues Thr180/Tyr182, while all forms of p38 are detected by a p38 antibody that recognizes total p38 protein (bottom panels in A to D). Arrowheads, phosphorylated p38 MAPK; arrows, total p38 MAPK; h, h p.i.; Mk, mock-infected cells; Mk*, cells treated with UV-irradiated culture medium; UV, cells infected with the inoculum containing UV-irradiated MHV. The phospho-specific signal in each immunoblot was quantitated by densitometric scanning and normalized against each total protein. The increase in phosphorylation for each sample is denoted as the fold increase over the signal from the zero hour p.i. time point and is indicated below each lane.

MAPK was almost undetectable in both cells. No significant increase in the amount of phosphorylation of p38 occurred in L929 cells infected at an MOI of 20 (data not shown), whereas an increase in the amount of phosphorylated p38 occurred at 12 h p.i. with an MOI of 100 (Fig. 1B). The difference in the extent of p38 phosphorylation in these cell lines was not surprising because the kinetics of MAPK activation is cell type and stimulus specific. Among all cell types, J774.1 cells showed the maximum accumulation of phosphorylated p38, and hence we chose this cell line for all subsequent studies.

We next examined whether another SAPK, JNK, was also phosphorylated in MHV-infected J774.1 cells. The jnk genes are ubiquitously expressed as 46- and 54-kDa proteins due to differential processing of the 3′ coding region of the corresponding mRNAs; there are no known functional differences between the 46- and 54-kDa isoforms of the kinase (20). As shown in Fig. 2, two phosphorylated forms of JNK, p46 and p54, were detected at 6 h p.i. and accumulated continuously up to 12 h p.i. The kinetics of phosphorylated JNK accumulation in infected J774.1 cells was similar to that of the accumulation

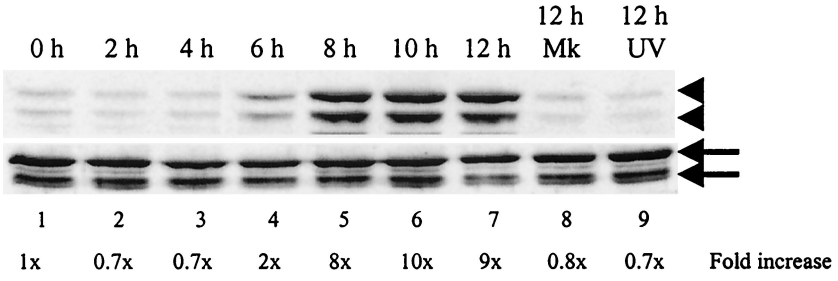

FIG. 2. JNK phosphorylation in MHV-infected cells. J774.1 cells were mock infected (Mk), MHV infected, or exposed to inoculum containing UV-irradiated MHV (UV). Cell lysates were harvested at the indicated times and analyzed by Western blot with a JNK phospho-specific antibody that detects JNK phosphorylated at residues Thr183 and Tyr185, shown in the upper panel (arrowheads), and a phosphorylation state-independent antibody that detects total JNK, shown in the lower panel (arrows). The upper arrow and upper arrowhead indicate JNK p54; the lower arrow and lower arrowhead indicate JNK p46.

of phosphorylated p38; JNK activation peaked at 8 to 10 h p.i., after which it declined to basal levels by 16 h p.i. (data not shown); an increase in the amount of both phosphorylated SAPKs was evident by 6 h p.i., and these SAPKs accumulated continuously for up to 12 h p.i. (see Fig. 1D and 2). In marked contrast, ERK1/2, which is usually activated by growth factors, hormones, and mitogens (5), was not phosphorylated in MHV-infected J774.1 cells (data not shown). These data showed that both SAPKs, p38 and JNK, were phosphorylated in MHV-infected cultured cells.

MHV replication is required for p38 and JNK MAPK phosphorylation. To determine whether MHV replication was required for p38 MAPK phosphorylation, we used a UV light-irradiated virus sample. Culture fluid from both MHV-infected DBT cells and mock-infected DBT cells was collected at 20 h p.i. and exposed to UV light (wavelength, 253 nm) for 20 min. UV irradiation was omitted in the control samples. UV-irradiated samples had an infectivity of less than 1 PFU/ml. J774.1 cells were infected with an unirradiated or irradiated virus samples or left untreated for 12 h p.i. Phosphorylated p38 did not increase in samples inoculated with the UV-irradiated virus sample (Fig. 1D, lane 14), the UV-irradiated DBT culture fluid sample (Fig. 1D, lane 13), and the unirradiated DBT culture fluid sample (data not shown). UV-irradiated MHV also failed to phosphorylate p38 MAPK in 17Cl-1 and DBT cells (Fig. 1A, lane 7, and 1C, lane 13). Furthermore, J774.1 cells that were exposed to UV-irradiated MHV failed to phosphorylate JNK as well (Fig. 2, lane 9). Together, these results demonstrated that MHV replication was required for p38 and JNK MAPK phosphorylation and eliminated the possibility that attachment of MHV to cell surface receptors alone or other factors present in the virus inoculum were responsible for p38 and JNK MAPK phosphorylation in infected cells.

Phosphorylated p38 MAPK in infected cells is biologically functional. To establish that MHV-induced p38 MAPK phosphorylation represented a biologically active kinase, we tested whether phosphorylated p38 found in MHV-infected cells could phosphorylate its downstream substrate, ATF-2, in an in vitro kinase assay (28), which examined whether immunoprecipitated phosphorylated p38 can phosphorylate ATF-2 in vitro; Western blot analysis, with ATF-2-phospho-specific antibody, revealed the status of ATF-2 phosphorylation. As shown in Fig. 3, immunoprecipitated phosphorylated p38 obtained at 0 h p.i. showed very low levels of ATF-2 phosphorylation activity, whereas this activity was slightly higher at 4 h p.i. The phosphorylated p38 that was isolated at 8 h p.i could efficiently phosphorylate ATF-2 in vitro, suggesting that phosphorylated p38 in infected cells was biologically active.

To confirm that the ATF-2 phosphorylation was specifically mediated by p38 MAPK, a p38-specific inhibitor, SB 203580, was added to the in vitro kinase reaction. For this analysis, we used 400 μg of lysate, which was twice the amount of lysate used in the experiments described above, as the initial material. After immunoprecipitation of phosphorylated p38, the sample was divided into two groups; one was resuspended in buffer containing 20 μM SB 203580, and the other was resuspended in buffer containing an equivalent volume of DMSO, which was used to dissolve SB 203580. The samples were incubated on ice for 10 min before initiating the kinase reaction. The addition of SB 203580, but not of DMSO, dramatically reduced the phosphorylation of ATF-2 (Fig. 3, lanes 4 and 5), clearly demonstrating that ATF-2 phosphorylation was mediated by p38 MAPK. The phosphorylated p38 MAPK that accumulated in MHV-infected cells was a biologically active kinase.

Activation of the upstream kinase, MKK3, during MHV infection. The p38 MAPKs are directly activated by MKKs (44, 45). MKK3 and MKK6, which share 80% homology, have been implicated as the major upstream activators of p38 MAPK both in vivo and in vitro (8). To determine how p38 MAPK was

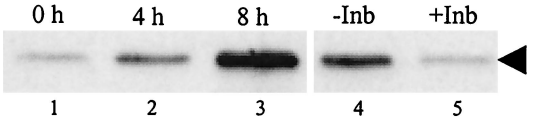

FIG. 3. Kinase activity of MHV-induced phosphorylated p38 in vitro. Cell extracts were prepared from MHV-infected J774.1 cells at the indicated times p.i. (lanes 1 to 3). For lanes 1 to 3, lysates were immunoprecipitated with p38-phospho-specific antibody and the p38 kinase activity of the immunecomplex was determined by using recombinant ATF-2 as the substrate in an in vitro kinase assay. Kinase reactions were analyzed by Western blot with an ATF-2-phospho-specifc antibody that detects ATF-2 phosphorylated at Thr71. For lanes 4 and 5, protein lysates that were extracted at 8 h p.i. were used for immunoprecipitation. "−Inb" and "+Inb" refer to immunoprecipitated complexes that were treated with DMSO and 20 μM SB 203580, respectively, prior to adding ATF-2 substrate. The arrowhead denotes phosphorylated ATF-2.

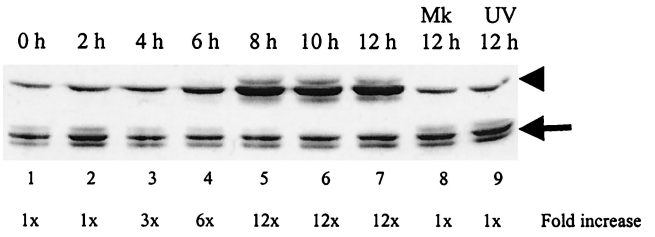

FIG. 4. MKK3 phosphorylation in MHV-infected cells. J774.1 cells were mock infected (Mk), MHV infected, or exposed to inoculum containing UV-irradiated MHV (UV). Cell lysates were harvested at the indicated times and analyzed by Western blot with an MKK3/6 phospho-specific antibody that detects MKK3/6 phosphorylated at Ser189/207, shown in the upper panel (arrowhead), or with a phosphorylation-state-independent antibody that detects total MKK3 alone (not MKK6), shown in the lower panel (arrow).

activated in MHV-infected cells, we examined the phosphorylation status of MKK3/6 in infected cells. If MKK3/6 are phosphorylated in infected cells, then they are most probably responsible for p38 activation. In contrast, if MKK3/6 are not activated in infected cells, then it is possible that one (or multiple) MHV-specific protein(s) is directly responsible for activating p38. Protein lysates from MHV-infected J774.1 cells were analyzed by Western blot analysis, with MKK3/6 phospho-specific antibodies that recognize phosphorylated MKK3 on Ser189 and phosphorylated MKK6 on Ser207 (Fig. 4). Phosphorylated MKK3/6 began to accumulate at 6 h p.i. and maximal phosphorylation occurred between 8 to 12 h p.i. The accumulation kinetics of phosphorylated MKK3/6 and that of phosphorylated p38 MAPK were similar (Fig. 1D). Mock-infected cells, harvested at 12 h p.i., showed no accumulation of phosphorylated MKK3/6. Cells exposed to the UV-irradiated virus sample also failed to phosphorylate MKK3/6 (Fig. 4, lane 9). Western blot analysis with a phosphorylation-state-independent anti-MKK3 antibody revealed the presence of MKK3 in J774.1 cells (Fig. 4, bottom panel), whereas a phosphorylation-state-independent antibody that reacted with only MKK6 failed to demonstrate the presence of MKK6 in this cell line (data not shown), strongly suggesting that J774.1 cells expressed only MKK3 and not MKK6. Taken together, these data showed that MHV infection induced the activation of the upstream kinase MKK3 and that activated MKK3 most likely accounted for the phosphorylation and activation of p38 MAPK.

MHV-induced p38 MAPK activation results in IL-6 secretion. The p38 MAPK pathway plays an essential role in the biosynthesis of proinflammatory cytokines, such as tumor necrosis factor alpha and IL-6, in many different cell types through the regulation of transcriptional and translational events (34, 35). To examine the biological consequence of MHV-induced p38 MAPK activation, we explored whether activated p38 MAPK resulted in the synthesis and secretion of IL-6 in infected J774.1 cells. Several pyridinyl imidazole compounds, such as SB 203580, are specific inhibitors of p38 MAPK and are known to block the production of proinflammatory cytokines such as IL-6 (35). Because SB 203580 blocks activated p38 MAPK function, a direct role of activated p38 in the putative production of IL-6 could be examined by adding SB 203580 to infected cultures.

As a first step, we used the LDH release assay to examine the viability of J774.1 cells treated with SB 203580. The LDH release assay measures the amount of LDH released into the cell culture media after the cells are treated with different concentrations of SB 203580. The amount of LDH released is directly proportional to the integrity of the cell membrane and hence is a measure of cell viability. J774.1 cells were treated with 20 and 50 μM SB 203580 or with DMSO alone (since DMSO was used to dissolve SB 203580) for 24 h. Untreated cells were used as controls. Culture supernatants were clarified by centrifugation and used to assay the amount of LDH released. Using the untreated cells as controls, we calculated the percentage of viable cells remaining after treatment as described in Materials and Methods. Treating cells with up to 50 μM SB 203580 had little effect on cell viability (data not shown). Hence, treating cells with 20 μM SB 203580 was not detrimental to the cells, and since this drug concentration is known to efficiently block p38 MAPK activity in vivo (6), we used 20 μM SB 203580 in subsequent experiments.

We used an RNase protection assay to examine whether IL-6-specific mRNAs were synthesized in infected cells. Intracellular RNAs were extracted at 4, 8, 12, and 16 h p.i. from MHV-A59-infected J774.1 cells. The RNA samples were hybridized with radiolabeled murine cytokine-specific mRNAs (Pharmingen RPA probe set mCK-2b). Mock-infected cells served as controls. We found an increased amount of IL-6 mRNAs at 8 h p.i. (data not shown). The amount of IL-6 mRNAs increased continuously until 16 h p.i.; the amount of IL-6 mRNAs increased by ~2-fold at 16 h p.i. compared to the amount observed at 4 h p.i. In contrast, accumulation of IL-6 mRNAs did not occur in mock-infected cells. (data not shown). To examine IL-6 production in infected cells, culture supernatants from DMSO-treated, MHV-infected J774.1 cells and from SB 203580-treated, MHV-infected J774.1 cells were harvested at 24 h p.i. After removal of the cell debris, clarified culture fluids were used for an ELISA assay to determine the release of IL-6. About 200 to 250 pg of IL-6/ml was produced by the DMSO-treated, MHV-infected J774.1 cells, whereas treatment with SB 203580 reduced the release of IL-6 by 85% (Fig. 5). DMSO-treated, mock-infected cells produced a basal level of IL-6. These results were consistent in three independent experiments, demonstrating that one of the biological consequences of p38 MAPK activation in MHV-infected cells was the synthesis and release of IL-6.

Role of p38 MAPK in activating the Mnk1-eIF4E pathway in infected cells. Activation of either ERKs or p38 MAPK results in the phosphorylation of a translation initiation factor, eIF4E (43, 46). The crystal structure of eIF4E suggested that phosphorylation of the molecule on Ser209 could result in a stronger affinity of phosphorylated eIF4E for capped mRNAs (12, 40). However, the exact mechanism whereby eIF4E phosphorylation results in increased rates of cap-dependent translation is still unknown. A recent study determined that Mnk1 is a substrate for activated p38 MAPK, and phosphorylated Mnk1 serves as the biologically relevant kinase for eIF4E in vivo (10, 64, 65). MHV infection results in strong inhibition of host protein synthesis concomitant with increased viral protein synthesis (15, 54, 59). We wondered whether activation of the p38 MAPK in MHV-infected cells results in the activation of the

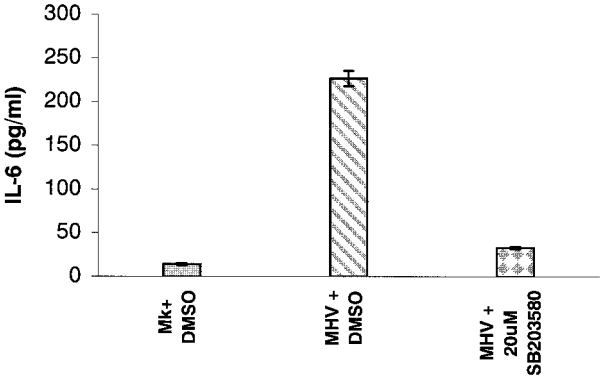

FIG. 5. MHV-induced p38 MAPK activation-dependent IL-6 secretion. Mock-infected J774.1 cells (Mk+DMSO) or MHV-infected J774.1 cells were incubated in the presence of DMSO (MHV+DMSO) or 20 μM SB 203580 (MHV+20 μM SB 203580). ELISA was used to determine the amount of IL-6 present in culture fluid at 24 h p.i. Error bars indicate the standard deviation from experimental points in triplicate determinations.

Mnk1-eIF4E pathway, which contributes to efficient MHV-specific protein synthesis.

At first we determined the phosphorylation status of Mnk1 in infected cells. Cell extracts were prepared from MHV-infected J774.1 cells at various times p.i. Equal amounts (30 μg) of lysates were analyzed by Western blot analysis, with a Mnk1 phospho-specific antibody that detects Mnk1 phosphorylated on Thr197/202. The immunoblots were subsequently reprobed with a phosphorylation-state-independent antibody that served as a loading control. There was no phosphorylated Mnk1 signal at 0 h p.i., probably due to very low, underdetectable levels of the active kinase at this time point. There is very little documentation regarding the basal levels of phosphorylation of Mnk1 in unstimulated cells. Scheper et al. have suggested that Mnk1 has very low basal levels of phosphorylation which increase only upon stress signaling (49). Hence, the underdetectable levels of phosphorylated Mnk1 signal at 0 h and 4 h p.i. (when the signaling cascade is not activated) were not surprising or unexpected. However, by 8 h p.i., consistent with p38 activation in this cell line, Mnk1 phosphorylation occurred (Fig. 6, lane 3). Increased Mnk1 phosphorylation was detected up to 10 h p.i., even though the phosphorylation signal dropped slightly after 8 h p.i. (Fig. 6, lane 5). An unknown protein, marked with an asterisk, migrated at a slightly slower rate than did Mnk1 (Fig. 6). This band appeared with similar intensity in all of the lanes. These data demonstrated that Mnk1 was phosphorylated in MHV-infected cells with kinetics mirroring that of p38 MAPK activation. To determine whether this Mnk1 activation was regulated by the activated p38 MAPK, MHV-infected J774.1 cells were treated with the p38-specific inhibitor, SB 203580, for various times p.i., and intracellular protein lysates from these samples were analyzed by Western blot with the phospho-specific Mnk1 antibody. As shown in Fig. 6, treating infected cells with SB 203580 almost completely abrogated Mnk1 phosphorylation. As a negative control, UV-irradiated virus-infected cells were analyzed for Mnk1 phosphorylation, but no such phosphorylation increases were seen (Fig. 6, lane 7). Therefore, Mnk1 phosphorylation required active MHV replication and most probably resulted from the activation of the p38 MAPK pathway. Besides the increased secretion of IL-6, another downstream event of p38 MAPK activation in MHV-infected cells was the phosphorylation and activation of Mnk1 kinase. To our knowledge this is the first demonstration of Mnk1 kinase activation due to viral infection.

Because Mnk1 is known to directly activate eIF4E to increase cap-dependent translation (12, 64), we also assessed the phosphorylation status of eIF4E in MHV-infected cells. Equal amounts (30 μg) of cell extracts were prepared from MHV-infected J774.1 cells at various times p.i., and the lysates were analyzed by Western blot with an eIF4E phospho-specific antibody that detects eIF4E phosphorylated at Ser209. The immunoblots were subsequently reprobed with a phosphorylation-state-independent antibody that served as a loading control. At the time of infection (0 h p.i.), a low basal level of phosphorylated eIF4E was detected and was of an amount commonly found in growing cells (63, 64) (Fig. 7A). At 4 h p.i. there was a slight decrease in eIF4E phosphorylation, and this reduction consistently occurred in four independent experiments. However, we do not know the reason or the significance of the decrease in eIF4E phosphorylation early in infection. Coincident with p38 MAPK and Mnk1 activation kinetics, the amount of phosphorylated eIF4E increased by 2.5-fold from 4 to 8 h p.i., and the elevated level of phosphorylated eIF4E was maintained at 10 h p.i. (Fig. 7A, lanes 3 and 4). The increase in eIF4E phosphorylation from 4 h p.i. to 8 to 10 h p.i. was consistently seen in four independent experiments. We assessed, as a negative control, the phosphorylation of eIF4E in cells infected with UV-irradiated virus, since the UV-inactivated virus did not activate p38 MAPK (Fig. 1). The levels of phosphorylated eIF4E in uninfected cells and in UV-irradiated virus-infected cells at 10 h p.i. were compared with those at 0 h p.i. and were determined to be similar (Fig. 7A, lanes 5 and 6). Active MHV replication was required to induce the enhanced phosphorylation of eIF4E.

eIF4E is one of the key components of translation initiation, and its phosphorylation status is subject to several regulators (12). To determine whether activation of the p38 MAPK pathway resulted in eIF4E phosphorylation in MHV-infected cells, we examined the effect of suppression of p38 MAPK activation on eIF4E phosphorylation. MHV-infected J774.1 cells were incubated in the presence of DMSO or SB 203580. At various

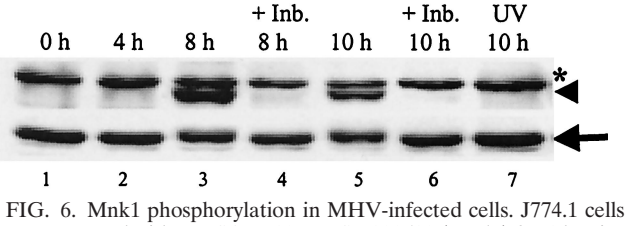

FIG. 6. Mnk1 phosphorylation in MHV-infected cells. J774.1 cells were pretreated with DMSO or 20 μM SB 203580 (+Inb.) for 1 h prior to MHV infection. Then cells were infected with MHV or UV-irradiated MHV (UV) for 1 h. The virus inoculum was removed, and the cells were kept continuously in the presence of DMSO or SB 203580 (+Inb.). At the indicated times p.i., lysates were prepared and 30-μg protein lysates were analyzed by Western blot with a Mnk1 phospho-specific antibody, shown in the upper panel (arrowhead), that detects Mnk1 phosphorylated at Thr197/202 and with a phosphorylation-state-independent antibody, shown in the lower panel (arrow), that detects total Mnk1. The asterisk represents a nonspecific protein band.

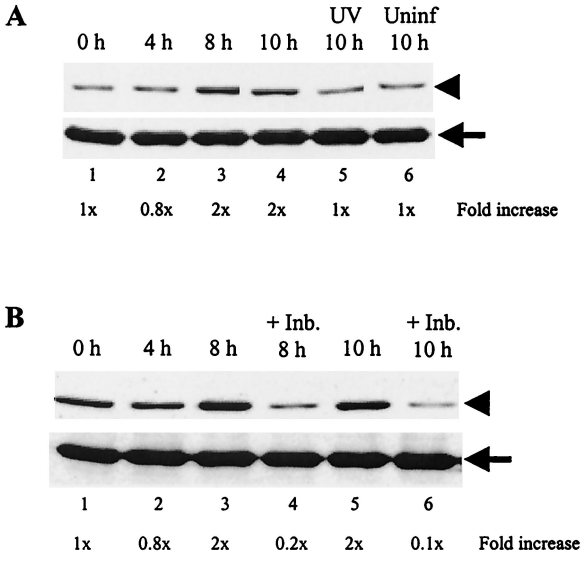

FIG. 7. Accumulation of phosphorylated eIF4E in MHV-infected cells. (A) J774.1 cells were left uninfected (Uninf), MHV infected, or exposed to inoculum containing UV-irradiated MHV (UV). At the times indicated, cell lysates were prepared and 30-μg protein lysates were analyzed by Western blot analysis with eIF4E phospho-specific antibody that detects eIF4E phosphorylated at Ser209, shown in the upper panel. The blots were subsequently stripped and reprobed with an eIF4E antibody that recognizes all forms of eIF4E (shown in the lower panel). The arrowhead and arrow denote phosphorylated eIF4E and total eIF4E, respectively. (B) J774.1 cells were pretreated with DMSO or 20 μM SB 203580 (+Inb.) for 1 h prior to MHV infection. Cells were then infected with MHV for 1 h. After the virus inoculum was removed, the cells were kept continuously in the presence of DMSO or SB 203580 (+Inb.). At the indicated times p.i., lysates were prepared and Western blot analysis was performed as described in panel A. The increase in the phospho-specific signal, normalized against the total protein signal and expressed as a fold increase over the zero hour p.i. signal, is indicated below each lane.

times p.i., cell extracts were prepared and the status of eIF4E phosphorylation was examined. Representative data from four independent experiments are shown in Fig. 7B. In this set of experiments, at the time of infection, the basal level of phosphorylated eIF4E was slightly higher at 0 h p.i. (Fig. 7B, lane 1). Consistent with the data shown in Fig. 7A, we observed a slight decrease in phosphorylated eIF4E levels at 4 h p.i. and an increase in phosphorylated eIF4E levels at 8 and 10 h p.i. (Fig. 7B), whereas phosphorylated eIF4E amounts were clearly reduced in SB 203580-treated, MHV-infected cells at 8 and 10 h p.i. (Fig. 7B, lanes 4 and 6).

The data in Fig. 6 and 7 suggested that SB 203580 blocked the phosphorylation of Mnk1 by p38 MAPK, which in turn resulted in a lower phosphorylation of eIF4E. In addition, SB 203580 could also have affected the eIF4E-specific phosphatase by increasing its activity, possibly resulting in further lowering of phosphorylated eIF4E levels, below the basal level, in SB 203580-treated, MHV-infected cells at 8 and 10 h p.i. (Fig. 7). Taken together, our data suggested that MHV infection induced activation of Mnk1 and a transient phosphorylation of eIF4E, both of which were sensitive to the p38-specific inhibitor, SB 203580.

Inhibition of p38 MAPK pathway activation suppresses MHV production. We next studied whether p38 MAPK activation had any effect on MHV replication. We first examined the effect of p38 MAPK activation inhibition on MHV yield from infected cells. MHV-infected J774.1 cells were treated continuously with either DMSO or 20 μM SB 203580. Culture supernatants were collected at various times p.i., and the titer of the released MHV was determined by plaque assay (Fig. 8). We conducted these experiments twice and obtained similar results each time. Representative data from one of the experiments are shown in Fig. 8. The one-step growth kinetics of MHV production in the J774.1 cells were similar to those in other MHV-infected cell lines (39, 56). At 4 h p.i. the amounts of infectious MHV particles produced were similar in SB 203580-treated and DMSO-treated, MHV-infected cells, demonstrating that pretreating J774.1 cells with SB 203580 or DMSO did not affect virus binding to MHV receptors, viral uncoating steps, and the establishment of infection. There was an approximately 80% decrease in the production of infectious MHV from SB 203580-treated cells compared to those produced from DMSO-treated cells from 8 to 16 h p.i. At 26 h p.i., virus titer in SB 203580-treated cells was about one-half of that in DMSO-treated cells. As stated earlier, a lower level of MHV production in SB 20350-treated cells was not due to cytotoxic effect of SB 203580 on these cells. Specific inhibition of p38 MAPK activity resulted in a significant reduction of virus production, demonstrating that p38 MAPK activation affected MHV replication.

Effect of p38 MAPK activation on synthesis of MHV-specific proteins and mRNAs. To understand how p38 MAPK activation facilitated efficient MHV replication, the effect of p38 MAPK inhibition on MHV-specific protein synthesis was tested. MHV-infected J774.1 cells were radiolabeled with Tran^{35}S-label for 30 min in the presence or absence of SB 203580 at 4, 6, and 10 h p.i. SDS-PAGE analysis of cell extracts obtained at 4 h p.i. showed very similar ^{35}S-methionine-cysteine incorporation in the SB 203580-treated and untreated samples (Fig. 9A, lanes 1 and 2). This result was expected because p38 MAPK was not activated at 4 h p.i. Analysis of cell extracts at 6 and 10 h p.i. revealed a reduction in ^{35}S-methio-

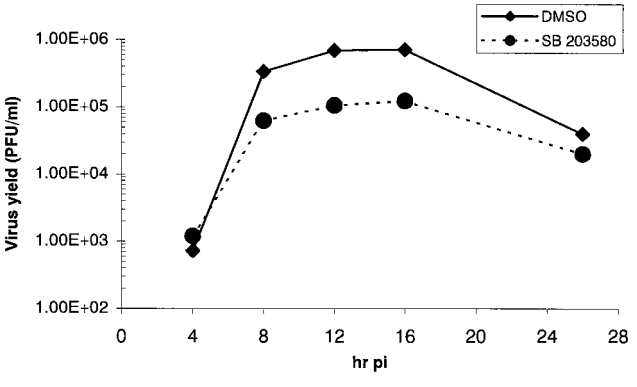

FIG. 8. Effect of p38 MAPK activation on MHV production. J774.1 cells that were pretreated with DMSO or 20 μM SB 203580 for 1 h were infected with MHV for 1 h. After removal of the inoculum, the cells were continuously treated with DMSO (◆) or 20 μM SB 203580 (●). The release of infectious MHV into the supernatant at the indicated times p.i. was determined by plaque assay.

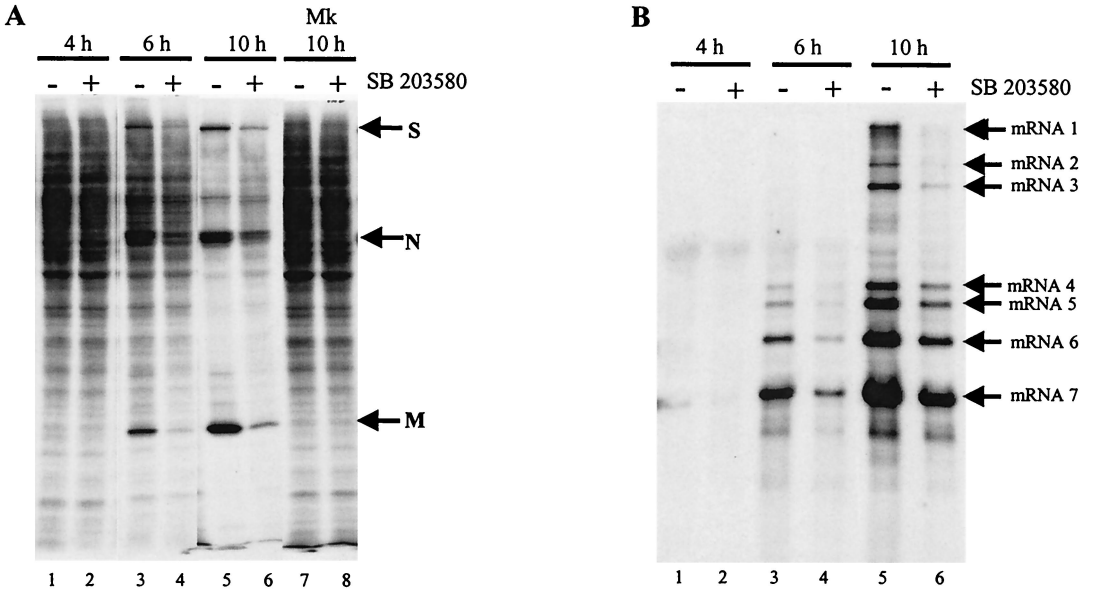

FIG. 9. Effect of p38 MAPK activity inhibition on translation (A) and virus-specific mRNA transcription (B). (A) J774.1 cells were left untreated (−) or were treated with 20 μM SB 203580 (+) for 1 h prior to infection. Cells were mock (Mk) or MHV infected. After 1 h of incubation, the inoculum was replaced with medium either lacking (−) or containing (+) 20 μM SB 203580. The culture medium was replaced with methionine-cysteine-free medium lacking (−) or containing (+) 20 μM SB 203580 1 h prior to each indicated time point. After 30 min of incubation, 75 μCi of Tran^{35}S-label/ml was added to the culture medium. After 30 min of additional incubation, cell extracts were prepared and one-half of each sample was analyzed by SDS–12% PAGE. The positions of the MHV structural proteins S, N, and M are indicated by arrows. (B) Intracellular RNA was extracted from the remaining half of the lysates described above. After RNA was separated on a 1% agarose-formaldehyde gel, the RNAs were transferred to a nylon membrane. Northern blot analysis was performed with a random-primed DIG-labeled probe, specific for all MHV mRNAs. The positions of the MHV-specific mRNAs mRNA1 to mRNA7 are indicated with arrows.

nine-cysteine incorporation, particularly into the MHV-specific proteins S, N, and M, in SB 203580-treated cells compared to untreated cells (Fig. 9A). The kinetics of MHV-specific protein accumulation in infected J774.1 cells in the absence of SB 203580 and those in other infected cell lines were similar (3, 15, 54). As shown above, p38 MAPK activation started to occur at 6 h p.i. and attained a maximum level at 8 to 10 h p.i. (Fig. 1). The low level of host protein synthesis at 10 h is due to a poorly understood MHV-induced host protein synthesis inhibition (15, 59, 60). Continuous incubation of mock-infected cells with SB 203580 for up to 10 h p.i. had no effect on the translation of cellular proteins (Fig. 9A, lane 8). These data demonstrated that activated p38 MAPK increased the translation of virus-specific proteins.

We next examined the effect of p38 MAPK inhibitor on the accumulation of viral transcripts in infected J774.1 cells. Northern blot analysis of intracellular RNAs showed a low level of MHV-specific mRNAs at 4 h p.i. (Fig. 9B), and these accumulated in infected cells by 6 h p.i.; further, there was a clear reduction in the amount of accumulated MHV mRNAs in the presence of SB 203580 (Fig. 9B, lanes 3 and 4). At 10 h p.i., the amount of MHV-specific mRNAs in SB 203580-treated cells was approximately one-third that of untreated cells. These data were reproducible in three independent experiments and demonstrated that inhibition of p38 MAPK activity also resulted in a severe reduction in the accumulation of viral-specific mRNAs in infected cells. The inhibition of MHV-specific protein synthesis and mRNA accumulation by treatment with SB 203580 late in infection was most likely a reason for the reduced MHV production in the presence of SB 203580.

DISCUSSION

Virus-induced alterations in cellular functions and/or behavior during infection have a profound impact on both cell viability and pathogenesis of the virus. However, little is known about the effect of viruses, especially RNA viruses, on such altered cellular functions. Here we report a study of the cellular mechanisms by which MHV caused the activation of physiologic intracellular signaling cascades that led to the phosphorylation and activation of downstream molecules. We showed that MHV infection of permissive cells stimulated both p38 MAPK and JNK/SAPK pathways but not the activation of ERK1/2, a third member of the major MAPK pathways, suggesting that only the SAPKs were activated in MHV-infected cells. Since phosphorylation of p38 MAPK and JNK occurred in four different MHV-permissive cell lines, activation of MAPK was not cell type specific. Activation of p38 MAPK and JNK did not occur in cells exposed to MHV inoculum that were inactivated by UV irradiation prior to infection, demonstrating that binding of the virus to cell surface receptors or other unidentified substances, which might be present in the inoculum, did not cause MAPK activation. We also observed the activation of MKK3 in infected cells, indicating that the upstream kinase responsible for p38 activation was MKK3. The phosphorylated p38 MAPK was a biologically functional molecule because it phosphorylated its downstream substrate,

ATF-2, in an in vitro kinase assay. Furthermore, we identified two downstream events regulated by p38 MAPK activation. One was the synthesis and secretion of the proinflammatory cytokine, IL-6, and the other was the activation of Mnk1 kinase resulting in the transient phosphorylation of eIF4E. In addition, the production of infectious MHV was reduced in cells in which p38 MAPK activity was blocked, which suggests that activation of this signaling cascade was important for MHV production.

McGilvray et al. reported the activation of both p38 MAPK and ERK in peritoneal exudative macrophages exposed to MHV-3 (41). These authors further demonstrated that MHV-3-induced p38 MAPK activation occurs within 1 to 5 min of infection and that UV-irradiated MHV-3 can phosphorylate p38 MAPK. In the present study, MHV-A59 infection did not activate ERK pathway in two different cells lines and p38 MAPK activation started much later, at 6 h p.i. Furthermore, UV-irradiated MHV failed to phosphorylate p38 MAPK. The p38 MAPK activation reported by McGilvray et al. seems to be an immediate-early response elicited by virus binding to cell surface receptors. Also, their study could not rule out the possibility that some factor(s) present in the inoculum could induce both p38 MAPK and ERK activation. These differences between the two studies demonstrate the diversity in virus-induced MAPK activation pathways, in which the type and dose of the trigger and the cell type both determine the nature and outcome of the cellular response to virus infection.

The mechanism of MHV-induced p38 MAPK activation. Activation of MKK3, an upstream kinase of p38 MAPK, occurred in MHV-infected cells (Fig. 4). The kinetics of MKK3 and p38 MAPK activation were similar. Therefore, the upstream kinase that activates p38 MAPK in MHV-infected cells was most likely MKK3. The mechanism of MKK3 activation in infected cells, however, is unknown and requires further studies. Several MKKKs, such as MTK2, MLK2/3, and ASK1, lie upstream of MKK3 (45) and receive information from cell surface receptors or interact with small GTP-binding proteins of the Ras superfamily (48). Activation of p38 MAPK started at 6 h p.i. in infected J774.1 cells, and a UV-irradiated MHV inoculum failed to activate both p38 MAPK and MKK3 (Fig. 1 and 4). These data strongly argue against the binding of MHV to MHV receptors causing the activation of the p38 MAPK cascade shown in the present study. Because MHV replication was necessary for MKK3 and p38 MAPK activation, the accumulation of some viral products by 6 h p.i. may exceed a threshold concentration to directly activate MKK3 or its upstream pathway. Putative virus products include virus-specific proteins and viral RNAs. There is a precedent that accumulation of a virus-specific protein induces activation of a MAPK pathway; accumulation of the herpes simplex virus type 1 VP16 protein activates both p38 MAPK and JNK (69). A recent report showed that both the p38 MAPK and the JNK/SAPK pathways are activated after fibroblasts are treated with the synthetic dsRNA poly(I)-poly(C) (18); hence, MHV dsRNA intermediates that accumulate in infected cells may also trigger the p38 MAPK activation pathway.

An alternative mechanism for p38 MAPK pathway activation could be the virus-induced disruption of a cellular function activating MKK3 and/or its upstream pathway. Iordanov et al. showed that either chemical-induced or UV-light-induced sequence-specific damage to the 28S rRNA in cultured cells activates MAPK (19). We know that MHV infection causes extensive and specific cleavage of 28S rRNA, leaving the 18S rRNA intact (3). Hence, it is conceivable that MHV-induced 28S rRNA cleavage triggers p38 MAPK pathway activation. In addition, MHV-induced host protein synthesis inhibition (15, 53, 59) may activate the MAPK pathway; virus usurping the cellular translation machinery may exert stress and, consequently, the stress-activated response pathways could be triggered.

IL-6 production in MHV-infected cells via the p38 MAPK pathway activation. Several investigators reported that virus-induced p38 MAPK activation results in cytokine upregulation (13, 18, 27, 50). The proinflammatory cytokine IL-6 was secreted from MHV-infected J774.1 cells, and its production was inhibited by SB 203580, demonstrating that MHV-induced p38 MAPK activation also led to the synthesis and secretion of IL-6 (Fig. 5). A high level of accumulated IL-6 mRNA late in infection was most probably one of the mechanisms for the IL-6 production in infected J774.1 cells. The situation was different in DBT cells. MAPK activation occurred in MHV-infected DBT cells (Fig. 1), whereas a very minute amount of IL-6 mRNAs accumulated at 16 h p.i. and no IL-6 protein was secreted at 24 h p.i. (S. Banerjee and S. Makino, unpublished data). Hence, p38 MAPK activation pathway-mediated IL-6 production in MHV-infected cells appears to be cell type specific. Another possible mechanism for IL-6 production in MHV-infected J774.1 cells is that activated p38 MAPK pathway leads to the stabilization of IL-6 mRNA. Recent studies have shown that activation of the p38 MAPK pathway somehow stabilized mRNAs that contained AU-rich elements in their 3′ region; IL-6 mRNA and other proinflammatory cytokine mRNAs contain this AU-rich element (7, 68). We found that the accumulation of MHV-specific mRNAs decreased when the p38 MAPK activation pathway was blocked (Fig. 9B). Do these data suggest that activation of the p38 MAPK pathway also stabilizes MHV-specific mRNAs? Although further studies are needed to test this possibility, closer examination of the 3′-end region of MHV mRNAs failed to show any consensus AU-rich element like those found on proinflammatory cytokines (data not shown).

Proinflammatory cytokines and chemokines are produced in MHV-infected mice (32, 57), and there is a strong correlation between their presence at the site of MHV replication and disease development; however, the exact role of these molecules in MHV-induced demyelination is still under investigation (33). It is quite possible that various MHV-infected cells in mice secrete cytokines and chemokines through virus-induced activation of p38 MAPK pathway. These cytokines and chemokines produced from the MHV-infected cells then work to modulate MHV-induced diseases.

Biological significance of p38 MAPK-mediated eIF4E phosphorylation in MHV infection. We observed an increase in the amount of phosphorylated eIF4E in MHV-infected cells (Fig. 7). Because treatment of infected cells with SB 203580 suppressed this effect (Fig. 7B), p38 MAPK pathway activation was responsible for the accumulation of phosphorylated eIF4E in MHV-infected cells. Furthermore, this transient phosphorylation of eIF4E in infected cells was most probably mediated by Mnk1, the only known, biologically relevant eIF4E kinase

(Fig. 6); we demonstrated Mnk1 phosphorylation at 8 h p.i. and suppression of Mnk1 phosphorylation by SB 203580 treatment (Fig. 6).

Upregulation of eIF4E phosphorylation in MHV-infected cells was in sharp contrast to dephosphorylation of eIF4E in cells infected with other viruses, including adenovirus (17), influenza virus (9), encephalomyocarditis virus (24), and poliovirus (24). A recent study demonstrated a decrease in the phosphorylation of eIF4E in cells expressing hepatitis C virus nonstructural protein NS5A (14). To our knowledge, our study is the first demonstration of upregulation of eIF4E phosphorylation in virus-infected cells.

Phosphorylated eIF4E has a higher affinity for cap structures at the 5′ ends of mRNAs and also for eIF4G, the large scaffolding protein (12, 47). Increased eIF4E phosphorylation usually results in enhanced translation rates (12). Accordingly, an increase in the amount of phosphorylated eIF4E in MHV-infected cells most probably affected protein synthesis in infected cells. Consistent with this notion, MHV-specific protein synthesis was decreased when infected cells were treated with SB 203580 (Fig. 9A). A straightforward interpretation of these data is that upregulation of eIF4E phosphorylation enhanced virus-specific protein synthesis. Since eIF4E phosphorylation was mediated by p38 MAPK activation, treating MHV-infected cells with the p38-specific inhibitor, SB 203580, blocked p38 MAPK activity, which resulted in decreased phosphorylation of eIF4E (probably due to reduced activation of Mnk1), reducing the translation of MHV-specific proteins. Synthesis of MHV gene 1 proteins, whose primary function is to produce viral RNAs (29, 31), was probably also suppressed in the presence of SB 203580. This putative reduction in the amount of gene 1 proteins may be a reason for the reduction of MHV mRNA accumulation in the SB 203580-treated cells (Fig. 9B).

In addition to the role of phosphorylated eIF4E for enhanced synthesis of MHV-specific proteins, p38 MAPK-mediated eIF4E phosphorylation may be an important mechanism for producing some host proteins in an environment where host protein synthesis is suppressed by virus-induced functions. Indeed, our data showing a high level of IL-6 production occurring under conditions of severe host protein synthesis inhibition, late in MHV infection, support this notion (Fig. 5); IL-6 protein synthesis was probably augmented by upregulation of eIF4E phosphorylation.

eIF4E phosphorylation may not always result in increased protein translation. Recently, Knauf et al. demonstrated that under physiological conditions serum-induced cap-dependent translation was negatively regulated by the overexpression of Mnk1/2, possibly via eIF4E phosphorylation (26). According to the proposed model of these authors, mitogens and growth factors stimulate pathways such as the phosphatidylinositol 3-kinase system, which act as positive regulators of translation, resulting in growth. At the same time, activation of the p38 MAPK or ERK pathways, via the same inducers, serves as a negative regulator, downregulating cap-dependent translation (26). Our present study did not investigate the status of the phosphatidylinositol 3-kinase system in MHV-infected cells. It is possible that MHV-induced activation of Mnk1 and phosphorylation of eIF4E could serve some purpose other than augmenting virus-specific protein synthesis. But since the model proposed by Knauf and colleagues was specific for mitogen-stimulated signaling, it is possible that virus-induced signaling could have different or even opposing results from that of mitogen-activated signaling.

p38 MAPK activation and MHV production. The effect of p38 MAPK on virus replication has been studied in a limited number of viruses. Treatment of herpes simplex virus type 1-infected cells with SB 203580 resulted in a decrease in viral titer (70). The authors of that study discussed the possibility that stimulation of p38 MAPK enhanced transcription of specific viral gene promoters that resulted in increased virus production (70). It has also been reported that human immunodeficiency virus type 1 production increased in p38 MAPK-activated cells (50). In that study, p38 MAPK activation resulted in IL-18 upregulation that in turn stimulated the production of tumor necrosis factor alpha and IL-6. The authors speculated that these cytokines may help to increase HIV production.

We showed that inhibition of p38 MAPK activity resulted in reduced MHV production (Fig. 8), suggesting that activation of p38 MAPK was beneficial to MHV replication. Our finding that treating MHV-infected cells with SB 203580 resulted in decreased synthesis of all of the virus-specific structural proteins demonstrated that activated p38 MAPK affected virus-specific protein synthesis. Because MHV-specific mRNA accumulation was also suppressed when p38 MAPK activation was inhibited (Fig. 9B), reduction in the accumulation of both viral genomic RNA and structural proteins probably caused a lowered production of infectious MHV particles in cells treated with SB 203580.

Van Oordt et al. recently reported that the MKK3/6-p38 MAPK cascade alters the subcellular distribution of hnRNP A1 by modulating its phosphorylation status (62); p38 MAPK-mediated phosphorylation of hnRNP A1 results in its accumulation in the cytoplasm. Interestingly, hnRNP A1 protein accumulates in the cytoplasm of MHV-infected cells (36). Although the biological role of hnRNP A1 in MHV RNA synthesis is controversial (51), studies by Lai and coworkers have shown that hnRNP A1 binds to MHV RNA and that it plays an important role in MHV RNA synthesis (36, 52). Because the p38 MAPK pathway was activated in MHV-infected cells, it is reasonable to speculate that the activation of the MKK3-p38 MAPK cascade in MHV-infected cells results in the phosphorylation of hnRNP A1 and that this phosphorylated hnRNPA1 subsequently accumulates in the infected cytoplasm. It would be interesting to know whether the reduction in MHV RNA synthesis in the presence of SB 203580 (Fig. 9B) was also due to the effect of the drug on the alteration of subcellular distribution and phosphorylation of hnRNP A1 in infected cells.

ACKNOWLEDGMENTS

We thank Fumihiro Taguchi, National Institute of Neuroscience, Tokyo, Japan, for the J774.1 cells.

This work was supported by Public Health Service grant AI29984 from the National Institutes of Health and in part by a John Sealy Memorial Endowment Fund Award. K.N. was supported by a McLaughlin fellowship.

REFERENCES

1. **An, S., C. J. Chen, X. Yu, J. L. Leibowitz, and S. Makino.** 1999. Induction of apoptosis in murine coronavirus-infected cultured cells and demonstration of E protein as an apoptosis inducer. J. Virol. **73:**7853–7859.

2. **An, S., A. Maeda, and S. Makino.** 1998. Coronavirus transcription early in infection. J. Virol. **72:**8517–8524.
3. **Banerjee, S., S. An, A. Zhou, R. H. Silverman, and S. Makino.** 2000. RNase L-independent specific 28S rRNA cleavage in murine coronavirus-infected cells. J. Virol. **74:**8793–8802.
4. **Baric, R. S., S. A. Stohlman, and M. M. Lai.** 1983. Characterization of replicative intermediate RNA of mouse hepatitis virus: presence of leader RNA sequences on nascent chains. J. Virol. **48:**633–640.
5. **Chang, L., and M. Karin.** 2001. Mammalian MAP kinase signalling cascades. Nature **410:**37–40.
6. **Cuenda, A., and D. R. Alessi.** 2000. Use of kinase inhibitors to dissect signaling pathways. Methods Mol. Biol. **99:**161–175.
7. **Dean, J. L., M. Brook, A. R. Clark, and J. Saklatvala.** 1999. p38 mitogen-activated protein kinase regulates cyclooxygenase-2 mRNA stability and transcription in lipopolysaccharide-treated human monocytes. J. Biol. Chem. **274:**264–269.
8. **Enslen, H., J. Raingeaud, and R. J. Davis.** 1998. Selective activation of p38 mitogen-activated protein (MAP) kinase isoforms by the MAP kinase kinases MKK3 and MKK6. J. Biol. Chem. **273:**1741–1748.
9. **Feigenblum, D., and R. J. Schneider.** 1993. Modification of eukaryotic initiation factor 4F during infection by influenza virus. J. Virol. **67:**3027–3035.
10. **Fukunaga, R., and T. Hunter.** 1997. MNK1, a new MAP kinase-activated protein kinase, isolated by a novel expression screening method for identifying protein kinase substrates. EMBO J. **16:**1921–1933.
11. **Garrington, T. P., and G. L. Johnson.** 1999. Organization and regulation of mitogen-activated protein kinase signaling pathways. Curr. Opin. Cell Biol. **11:**211–218.
12. **Gingras, A. C., B. Raught, and N. Sonenberg.** 1999. eIF4 initiation factors: effectors of mRNA recruitment to ribosomes and regulators of translation. Annu. Rev. Biochem. **68:**913–963.
13. **Griego, S. D., C. B. Weston, J. L. Adams, R. Tal-Singer, and S. B. Dillon.** 2000. Role of p38 mitogen-activated protein kinase in rhinovirus-induced cytokine production by bronchial epithelial cells. J. Immunol. **165:**5211–5220.
14. **He, Y., S. L. Tan, S. U. Tareen, S. Vijaysri, J. O. Langland, B. L. Jacobs, and M. G. Katze.** 2001. Regulation of mRNA translation and cellular signaling by hepatitis C virus nonstructural protein NS5A. J. Virol. **75:**5090–5098.
15. **Hilton, A., L. Mizzen, G. MacIntyre, S. Cheley, and R. Anderson.** 1986. Translational control in murine hepatitis virus infection. J. Gen. Virol. **67:** 923–932.
16. **Hirano, N., K. Fujiwara, and M. Matumoto.** 1976. Mouse hepatitis virus (MHV-2). Plaque assay and propagation in mouse cell line DBT cells. Jpn. J. Microbiol. **20:**219–225.
17. **Huang, J. T., and R. J. Schneider.** 1991. Adenovirus inhibition of cellular protein synthesis involves inactivation of cap-binding protein. Cell **65:**271–280.
18. **Iordanov, M. S., J. M. Paranjape, A. Zhou, J. Wong, B. R. Williams, E. F. Meurs, R. H. Silverman, and B. E. Magun.** 2000. Activation of p38 mitogen-activated protein kinase and c-Jun NH_2-terminal kinase by double-stranded RNA and encephalomyocarditis virus: involvement of RNase L, protein kinase R, and alternative pathways. Mol. Cell. Biol. **20:**617–627.
19. **Iordanov, M. S., D. Pribnow, J. L. Magun, T. H. Dinh, J. A. Pearson, S. L. Chen, and B. E. Magun.** 1997. Ribotoxic stress response: activation of the stress-activated protein kinase JNK1 by inhibitors of the peptidyl transferase reaction and by sequence-specific RNA damage to the alpha-sarcin/ricin loop in the 28S rRNA. Mol. Cell. Biol. **17:**3373–3381.
20. **Ip, Y. T., and R. J. Davis.** 1998. Signal transduction by the c-Jun N-terminal kinase (JNK): from inflammation to development. Curr. Opin. Cell Biol. **10:**205–219.
21. **Jagus, R., B. Joshi, and G. N. Barber.** 1999. PKR, apoptosis and cancer. Int. J. Biochem. Cell Biol. **31:**123–138.
22. **Karin, M.** 1998. Mitogen-activated protein kinase cascades as regulators of stress responses. Ann. N. Y. Acad. Sci. **851:**139–146.
23. **Kim, K. H., K. Narayanan, and S. Makino.** 1997. Assembled coronavirus from complementation of two defective interfering RNAs. J. Virol. **71:**3922–3931.
24. **Kleijn, M., C. L. Vrins, H. O. Voorma, and A. A. Thomas.** 1996. Phosphorylation state of the cap-binding protein eIF4E during viral infection. Virology **217:**486–494.
25. **Klumperman, J., J. K. Locker, A. Meijer, M. C. Horzinek, H. J. Geuze, and P. J. Rottier.** 1994. Coronavirus M proteins accumulate in the Golgi complex beyond the site of virion budding. J. Virol. **68:**6523–6534.
26. **Knauf, U., C. Tschopp, and H. Gram.** 2001. Negative regulation of protein translation by mitogen-activated protein kinase-interacting kinases 1 and 2. Mol. Cell. Biol. **21:**5500–5511.
27. **Kujime, K., S. Hashimoto, Y. Gon, K. Shimizu, and T. Horie.** 2000. p38 mitogen-activated protein kinase and c-jun-NH_2-terminal kinase regulate RANTES production by influenza virus-infected human bronchial epithelial cells. J. Immunol. **164:**3222–3228.
28. **Kyriakis, J. M., and J. Avruch.** 2001. Mammalian mitogen-activated protein kinase signal transduction pathways activated by stress and inflammation. Physiol. Rev. **81:**807–869.
29. **Lai, M. M.** 1990. Coronavirus: organization, replication and expression of genome. Annu. Rev. Microbiol. **44:**303–333.
30. **Lai, M. M., P. R. Brayton, R. C. Armen, C. D. Patton, C. Pugh, and S. A. Stohlman.** 1981. Mouse hepatitis virus A59: mRNA structure and genetic localization of the sequence divergence from hepatotropic strain MHV-3. J. Virol. **39:**823–834.
31. **Lai, M. M., and D. Cavanagh.** 1997. The molecular biology of coronaviruses. Adv. Virus Res. **48:**1–100.
32. **Lane, T. E., V. C. Asensio, N. Yu, A. D. Paoletti, I. L. Campbell, and M. J. Buchmeier.** 1998. Dynamic regulation of alpha- and beta-chemokine expression in the central nervous system during mouse hepatitis virus-induced demyelinating disease. J. Immunol. **160:**970–978.
33. **Lane, T. E., and M. J. Buchmeier.** 1997. Murine coronavirus infection: a paradigm for virus-induced demyelinating disease. Trends Microbiol. **5:**9–14.
34. **Lee, J. C., S. Kumar, D. E. Griswold, D. C. Underwood, B. J. Votta, and J. L. Adams.** 2000. Inhibition of p38 MAP kinase as a therapeutic strategy. Immunopharmacology **47:**185–201.
35. **Lee, J. C., J. T. Laydon, P. C. McDonnell, T. F. Gallagher, S. Kumar, D. Green, D. McNulty, M. J. Blumenthal, J. R. Heys, S. W. Landvatter, et al.** 1994. A protein kinase involved in the regulation of inflammatory cytokine biosynthesis. Nature **372:**739–746.
36. **Li, H. P., X. Zhang, R. Duncan, L. Comai, and M. M. Lai.** 1997. Heterogeneous nuclear ribonucleoprotein A1 binds to the transcription-regulatory region of mouse hepatitis virus RNA. Proc. Natl. Acad. Sci. USA **94:**9544–9549.
37. **Locker, J. K., J. Klumperman, V. Oorschot, M. C. Horzinek, H. J. Geuze, and P. J. Rottier.** 1994. The cytoplasmic tail of mouse hepatitis virus M protein is essential but not sufficient for its retention in the Golgi complex. J. Biol. Chem. **269:**28263–28269.
38. **Makino, S., M. Joo, and J. K. Makino.** 1991. A system for study of coronavirus mRNA synthesis: a regulated, expressed subgenomic defective interfering RNA results from intergenic site insertion. J. Virol. **65:**6031–6041.
39. **Makino, S., F. Taguchi, M. Hayami, and K. Fujiwara.** 1983. Characterization of small plaque mutants of mouse hepatitis virus, JHM strain. Microbiol. Immunol. **27:**445–454.
40. **Marcotrigiano, J., A. C. Gingras, N. Sonenberg, and S. K. Burley.** 1997. Cocrystal structure of the messenger RNA 5′ cap-binding protein (eIF4E) bound to 7-methyl-GDP. Cell **89:**951–961.
41. **McGilvray, I. D., Z. Lu, A. C. Wei, A. P. Dackiw, J. C. Marshall, A. Kapus, G. Levy, and O. D. Rotstein.** 1998. Murine hepatitis virus strain 3 induces the macrophage prothrombinase fgl-2 through p38 mitogen-activated protein kinase activation. J. Biol. Chem. **273:**32222–32229.
42. **Mizutani, T., J. F. Repass, and S. Makino.** 2000. Nascent synthesis of leader sequence-containing subgenomic mRNAs in coronavirus genome-length replicative intermediate RNA. Virology **275:**238–243.
43. **Morley, S. J., and L. McKendrick.** 1997. Involvement of stress-activated protein kinase and p38/RK mitogen-activated protein kinase signaling pathways in the enhanced phosphorylation of initiation factor 4E in NIH 3T3 cells. J. Biol. Chem. **272:**17887–17893.
44. **Obata, T., G. E. Brown, and M. B. Yaffe.** 2000. MAP kinase pathways activated by stress: the p38 MAPK pathway. Crit. Care Med. **28:**N67–N77.
45. **Ono, K., and J. Han.** 2000. The p38 signal transduction pathway: activation and function. Cell Signal **12:**1–13.
46. **Pyronnet, S., H. Imataka, A. C. Gingras, R. Fukunaga, T. Hunter, and N. Sonenberg.** 1999. Human eukaryotic translation initiation factor 4G (eIF4G) recruits mnk1 to phosphorylate eIF4E. EMBO J. **18:**270–279.
47. **Rhoads, R. E.** 1999. Signal transduction pathways that regulate eukaryotic protein synthesis. J. Biol. Chem. **274:**30337–30340.
48. **Schafer, C., and J. A. Williams.** 2000. Stress kinases and heat shock proteins in the pancreas: possible roles in normal function and disease. J. Gastroenterol. **35:**1–9.
49. **Scheper, G. C., N. A. Morrice, M. Kleijn, and C. G. Proud.** 2001. The mitogen-activated protein kinase signal-integrating kinase Mnk2 is a eukaryotic initiation factor 4E kinase with high levels of basal activity in mammalian cells. Mol. Cell. Biol. **21:**743–754.
50. **Shapiro, L., K. A. Heidenreich, M. K. Meintzer, and C. A. Dinarello.** 1998. Role of p38 mitogen-activated protein kinase in HIV type 1 production in vitro. Proc. Natl. Acad. Sci. USA **95:**7422–7426.
51. **Shen, X., and P. S. Masters.** 2001. Evaluation of the role of heterogeneous nuclear ribonucleoprotein A1 as a host factor in murine coronavirus discontinuous transcription and genome replication. Proc. Natl. Acad. Sci. USA **98:**2717–2722.
52. **Shi, S. T., P. Huang, H. P. Li, and M. M. Lai.** 2000. Heterogeneous nuclear ribonucleoprotein A1 regulates RNA synthesis of a cytoplasmic virus. EMBO J. **19:**4701–4711.
53. **Siddell, S., H. Wege, A. Barthel, and V. ter Meulen.** 1981. Coronavirus JHM: intracellular protein synthesis. J. Gen. Virol. **53:**145–155.
54. **Siddell, S., H. Wege, A. Barthel, and V. ter Meulen.** 1981. Intracellular protein synthesis and the in vitro translation of coronavirus JHM mRNA. Adv. Exp. Med. Biol. **142:**193–207.
55. **Stark, G. R., I. M. Kerr, B. R. Williams, R. H. Silverman, and R. D.**

Schreiber. 1998. How cells respond to interferons. Annu. Rev. Biochem. **67:**227–264.
56. **Sturman, L. S., and K. K. Takemoto.** 1972. Enhanced growth of a murine coronavirus in transformed mouse cells. Infect. Immun. **6:**501–507.
57. **Sun, N., D. Grzybicki, R. F. Castro, S. Murphy, and S. Perlman.** 1995. Activation of astrocytes in the spinal cord of mice chronically infected with a neurotropic coronavirus. Virology **213:**482–493.
58. **Tahara, S., C. Bergmann, G. Nelson, R. Anthony, T. Dietlin, S. Kyuwa, and S. Stohlman.** 1993. Effects of mouse hepatitis virus infection on host cell metabolism. Adv. Exp. Med. Biol. **342:**111–116.
59. **Tahara, S. M., T. A. Dietlin, C. C. Bergmann, G. W. Nelson, S. Kyuwa, R. P. Anthony, and S. A. Stohlman.** 1994. Coronavirus translational regulation: leader affects mRNA efficiency. Virology **202:**621–630.
60. **Tahara, S. M., T. A. Dietlin, G. W. Nelson, S. A. Stohlman, and D. J. Manno.** 1998. Mouse hepatitis virus nucleocapsid protein as a translational effector of viral mRNAs. Adv. Exp. Med. Biol. **440:**313–318.
61. **Tooze, J., S. Tooze, and G. Warren.** 1984. Replication of coronavirus MHV-A59 in sac- cells: determination of the first site of budding of progeny virions. Eur. J. Cell Biol. **33:**281–293.
62. **van der Houven van Oordt, W., M. T. Diaz-Meco, J. Lozano, A. R. Krainer, J. Moscat, and J. F. Caceres.** 2000. The MKK(3/6)-p38-signaling cascade alters the subcellular distribution of hnRNP A1 and modulates alternative splicing regulation. J. Cell Biol. **149:**307–316.
63. **Wang, X., A. Flynn, A. J. Waskiewicz, B. L. Webb, R. G. Vries, I. A. Baines, J. A. Cooper, and C. G. Proud.** 1998. The phosphorylation of eukaryotic initiation factor eIF4E in response to phorbol esters, cell stresses, and cytokines is mediated by distinct MAP kinase pathways. J. Biol. Chem. **273:**9373–9377.
64. **Waskiewicz, A. J., A. Flynn, C. G. Proud, and J. A. Cooper.** 1997. Mitogen-activated protein kinases activate the serine/threonine kinases Mnk1 and Mnk2. EMBO J. **16:**1909–1920.
65. **Waskiewicz, A. J., J. C. Johnson, B. Penn, M. Mahalingam, S. R. Kimball, and J. A. Cooper.** 1999. Phosphorylation of the cap-binding protein eukaryotic translation initiation factor 4E by protein kinase Mnk1 in vivo. Mol. Cell. Biol. **19:**1871–1880.
66. **Wege, H., S. Siddell, and V. ter Meulen.** 1982. The biology and pathogenesis of coronaviruses. Curr. Top. Microbiol. Immunol. **99:**165–200.
67. **Weitzman, J. B., and M. Yaniv.** 1998. Signal transduction pathways and modulation of gene activity. Clin. Chem. Lab. Med. **36:**535–539.
68. **Winzen, R., M. Kracht, B. Ritter, A. Wilhelm, C. Y. Chen, A. B. Shyu, M. Muller, M. Gaestel, K. Resch, and H. Holtmann.** 1999. The p38 MAP kinase pathway signals for cytokine-induced mRNA stabilization via MAP kinase-activated protein kinase 2 and an AU-rich region-targeted mechanism. EMBO J. **18:**4969–4980.
69. **Zachos, G., B. Clements, and J. Conner.** 1999. Herpes simplex virus type 1 infection stimulates p38/c-Jun N-terminal mitogen-activated protein kinase pathways and activates transcription factor AP-1. J. Biol. Chem. **274:**5097–5103.
70. **Zachos, G., M. Koffa, C. M. Preston, J. B. Clements, and J. Conner.** 2001. Herpes simplex virus type 1 blocks the apoptotic host cell defense mechanisms that target Bcl-2 and manipulates activation of p38 mitogen-activated protein kinase to improve viral replication. J. Virol. **75:**2710–2728.